

1 ***CpALS4770 and CpALS4780 contribution to the virulence of *Candida****
2 ***parapsilosis***

3
4 Marina Zoppo^{a§*}, Mariagrazia Di Luca^a, Mauro Franco^{a§§}, Cosmeri Rizzato^b, Antonella
5 Lupetti^b, Annarita Stringaro^c, Flavia De Bernardis^d, Christoph Schaudinn^e, M. Inmaculada
6 Barrasa^f, Daria Bottai^a, Valmik K. Vyas^{f§§§} and Arianna Tavanti^a

7
8 ^a: Department of Biology, University of Pisa, Pisa, Italy

9 ^b: Department of Translational Research and New Technologies in Medicine and Surgery,
10 University of Pisa, Pisa, Italy

11 ^c: National Center for Drug Research and Evaluation, Italian National Institute of Health,
12 Rome, Italy.

13 ^d:Department of Infectious Diseases, Italian National Institute of Health, Rome, Italy.

14 ^e: Advanced Light and Electron Microscopy, Robert Koch Institute, Berlin, Germany

15 ^f: Whitehead Institute for Biomedical Research, Cambridge, MA 02142, USA

16
17 § Present address: Department of Environmental Toxicology Eawag, Dübendorf,
18 Switzerland

19 §§ Present address: Technische Universität Dresden, CRTD, Dresden, Germany

20 §§§ Present address: DSM Nutritional Products, Lexington, MA 02421, USA.

21
22
23
24 ***Corresponding author**

25 e-mail address: marina.zoppo@eawag.ch

26
27
28

1 **Abstract**

2

3

4 The ability of yeast to adhere to biotic and abiotic surfaces represents an essential trait
5 during the early stages of infection. Agglutinin-like sequence (Als) cell-wall proteins play
6 a key role in adhesion of *Candida* species. *Candida parapsilosis* genome encompasses 5
7 *ALS* members, of which only the role of *CPAR2_404800* has been elucidated. The present
8 project was aimed at investigating the contribution of *C. parapsilosis* Als proteins by
9 generating edited strains lacking functional Als proteins. *CPAR2_404770* and
10 *CPAR2_404780*, further indicated as *CpALS4770* and *CpALS4780*, were selected for the
11 generation of single and double edited strains using an episomal CRISPR/Cas9
12 technology. Phenotypic characterization of mutant strains revealed that editing of both
13 genes had no impact on the *in vitro* growth of *C. parapsilosis* or on morphogenesis.
14 Notably, *CpALS4770*-edited strain showed a reduction of biofilm formation and adhesive
15 properties to human buccal cells (HBECs). Conversely, single *CpALS4780*-edited strain
16 did not show any difference compared to the wild-type strain in all the assays performed,
17 while the double *CpALS4770-CpALS4780* mutant revealed an increased ability to produce
18 biofilm, a hyper-adhesive phenotype to HBECs, and a marked tendency to form cellular
19 aggregates. Murine vaginal infection experiments indicated a significant reduction in CFUs
20 recovered from BALB/c mice infected with single and double edited strains, compared to
21 those infected with the wild-type strain. These finding clearly indicate that *CpAls4770*
22 plays a role in adhesion to biotic and abiotic surfaces, while both *CpALS4770* and
23 *CpALS4780* genes are required for *C. parapsilosis* ability to colonize and persist in the
24 vaginal mucosa.

25

26

27

28 **Keywords:** *Candida parapsilosis*, episomal CRISPR/Cas9, Agglutinin-like sequence
29 (*ALS*) gene family, human buccal epithelial cells (HBECs), murine vaginal candidiasis.

30

1 1. INTRODUCTION

2

3 *Candida parapsilosis* is commonly associated with systemic fungal infections among
4 immunocompromised individuals, especially premature infants. Adhesion to host surfaces
5 is a key factor in pathogenesis, but this process has not been extensively studied in *non*
6 *albicans Candida* species. It is well known that *C. albicans* adhesion is mediated by a
7 number of cell wall proteins and among them, the agglutinin-like sequence (Als) proteins
8 are one of the best studied (Cota and Hoyer, 2015). Cross-hybridization analysis
9 comparing *C. albicans ALS* sequences and genomic DNA with other *Candida* species
10 suggested that similar genes are found in closely related fungi, including *C. parapsilosis*
11 where 5 putative *ALS* genes were identified (Hoyer et al., 2001; Butler et al., 2009).
12 Among these, the function of *CPAR2_404800 (CpALS4800)* has been investigated through
13 targeted gene disruption (Bertini et al., 2016) and the encoded adhesin has been
14 demonstrated to play a role in *C. parapsilosis* virulence and pathogenicity (Bertini et al.,
15 2016; Neale et al., 2018). Although a complete description of their structure and
16 nomenclature has recently been proposed (Oh et al., 2019), functions of the remaining Als
17 proteins in *C. parapsilosis* still need to be established.

18 The development of the CRISPR/Cas9 system as gene-editing technology has
19 revolutionized gene function studies in *Candida* research, allowing to rapidly generate
20 knock-outs and knock-ins in specific genetic *loci* and to simultaneously inactivate multiple
21 members of gene families (Enkler et al., 2016; Grahl et al., 2017; Norton et al., 2017;
22 Lombardi et al., 2019a; Zhu et al., 2019). The first evidence of the application of
23 CRISPR/Cas9 system for gene editing in *C. albicans* was developed in 2015 by Vyas *et*
24 *al.*(Vyas et al., 2015). This system was further improved in 2017, with the development of
25 an episomal CRISPR/Cas9 system for *C. parapsilosis* gene editing, with a self-processing
26 gRNA composed by the Hammerhead (HH) and hepatitis delta virus (HDV) ribozymes
27 (Gao and Zhao, 2014) under the regulation of a RNA polymerase II promoter (Lombardi et
28 al., 2017). Plasmid cure following the editing event allowed to minimize Cas9 expression,
29 and therefore, the likelihood of off-target events. The same group recently implemented
30 this system by replacing the HDV ribozyme with a tRNA sequence and used this approach
31 for the efficient gene editing in the *C. parapsilosis* species complex (Lombardi et al.,
32 2019a; Morio et al., 2019).

33 In the present work, the role of two uncharacterized *C. parapsilosis ALS* genes,
34 *CPAR2_404770* and *CPAR2_404780*, further referred as to *CpALS4770* and *CpALS4780*,

1 was investigated through the creation of single and double edited strains using the
2 ribozymes-based CRISPR/Cas9 system (Lombardi et al., 2017) described above. The panel
3 of mutant isolates was characterized for phenotypic traits such as growth rate, ability to
4 produce pseudohyphae, biofilm formation both on plastic surfaces and glass beads, and
5 adhesion on human epithelial buccal cells. Real-time RT PCR assay was used to evaluate
6 the transcriptional levels of *C. parapsilosis* *ALS* expression following *CpALS4770* and
7 *CpALS4780* inactivation. Finally, the pathogenic potential of the mutant collection was
8 assessed in a murine model of vaginal candidiasis.

10 **2. MATERIALS AND METHODS**

12 **2.1 *Candida parapsilosis* strain used in this study**

13 A highly adhesive clinical isolate of *C. parapsilosis*, CP50 (Bertini et al., 2013), was used
14 for the creation of single and multiple edited strains. Yeast cells were grown in YPD
15 medium at 30°C. Selection of edited clones was performed on YPD agar plates
16 supplemented with 100 µg/ml Nourseothricin (Nou, Werner BioAgents, Jena, Germany)
17 (YPD-Nou). Sabouraud Dextrose medium (1% mycological peptone, 2% dextrose, Sigma
18 Aldrich, Saint Louis, USA) (SAB) was used for morphology tests and biofilm formation
19 experiments.

21 **2.2 Computational design of guide RNA**

22 For each target gene, gRNA selection was performed according to a bioinformatics
23 analysis. We designed guide sequences corresponding to each annotated gene in the
24 genome of *C. parapsilosis*, using updated guide selection and scoring methods (Doench et
25 al., 2016). We listed all 20 nucleotides (nt) followed by NGG (or CCN plus 20 nt) in the
26 genome. We kept only the guides that were hitting the coding regions of genes. To find
27 putative off-targets, we took the 14 nt closest to the protospacer-adjacent-motif (PAM)
28 sequence, constructed the four possible sequences of the PAM, and mapped these with
29 Bowtie (<http://bowtie-bio.sourceforge.net/index.shtml>), allowing up to 3 mismatches. For
30 each original guide, we calculated the on-target score using rule set 2 for sgRNA on-target
31 activity script (described in Doench et al.(Doench et al., 2016)) as well as all the possible
32 off-target scores for all the places in the genome that the 14-nt NGG hit with ≤ 3
33 mismatches (cutting frequency determination [CFD] scoring) (Doench et al., 2016). Guides
34 were defined as having no off-targets if the off-target scores at other locations were lower

1 than 0.2. According to these criteria, 5' AAGCACAAAGGCAATAAACG 3' (- strand,
2 Cas9 cutting site far 31 nt from the beginning of the gene) and 5'
3 GGAGGCTCCAATACCAACCC 3' (+ strand, Cas9 cutting site 554 nt from the beginning
4 of the gene) were selected for *CpALS4770* and *CpALS4780* gene targeting, respectively.

5

6 **2.3 Construction of pSAT1-Ribo plasmid for *CpALS4770* and *CpALS4780* gene** 7 **editing**

8 The creation of *C. parapsilosis* edited strains relied on the use of the episomal
9 CRISPR/Cas9 system described in *C. parapsilosis* (Lombardi et al., 2017). Plasmids used
10 in this study, pUC57_HH_HDV_sgADE2B and pSAT1, were kindly provided by
11 Geraldine Butler, University College Dublin, Dublin. Plasmid
12 pUC57_HH_HDV_sgADE2B was linearized using primers GA7_pUC57F/GA7_pUC57R
13 (Supplementary Table 1). The selected gRNA sequences for *CpALS4770* and *CpALS4780*
14 gene editing were generated through primer extension using primers TOP-sgRNA-
15 Cp4770/BOTTOM-sgRNA-Cp4770 and TOP-sgRNA-CPAR2_4780/BOTTOM-sgRNA-
16 CPAR2_4780 (Supplementary Table 1) respectively, bearing 20 bp overlapping sequences
17 at the 3' ends. The resulting 100 bp DNA fragment and the linearized
18 pUC57_HH_HVD_sgADE2B plasmid were assembled together using Gibson Assembly®
19 Master Mix (New England Biolabs, Massachusetts, USA), according to manufacturer's
20 instructions. The resulting plasmids, harbouring the gRNA sequences specific for
21 *CpALS4770* and *CpALS4780* gene targeting, were respectively named
22 pUC57_RIBO_CpALS4770 and pUC57_RIBO_CpALS4780. The ribozyme cassette
23 encompassing the GAPDH promoter and terminator, the specific gRNA sequence, and the
24 HH-HDV ribozymes, was PCR amplified using primers GA_pSAT1_F/GA_pSAT1_R
25 (Supplementary Table 1). The amplified fragment was introduced by Gibson Assembly
26 into pSAT1 plasmid, previously linearized with NruI (New England Biolabs), thus
27 generating the final constructs, pRIBO-sgCpALS4770 and pRIBO-sgCpALS4780,
28 respectively.

29

30 **2.4 Repair template synthesis**

31 In order to introduce specific mutation in *CpALS4770* and *CpALS4780* gene sequences,
32 two different repair templates, further referred as RT-4770 and RT-4780, were generated
33 through primer extension. Primers RT_2xSTOP_CPAR2_4770 F/RT_2xSTOP
34 CPAR2_4770R and RT_2xSTOP_CPAR2_4780F/RT_2xSTOP CPAR2_4780R

1 (Supplementary Table 1) were used for *CpALS4770* and *CpALS4780* gene editing,
2 respectively. Each repair template generated had 40 bp homology regions arms at both
3 ends and a 12 bp insertion in the middle encompassing two stop codons (TAA, TAG) and
4 the KpnI restriction site.

5

6 **2.5 *C. parapsilosis* transformation and screening of recombinant clones**

7 Plasmids pRIBO-sgCpALS4770 and pRIBO-sgCpALS4780, harbouring the gRNA
8 specific for *CpALS4770* and *CpALS4780*, respectively, were transformed in *C. parapsilosis*
9 parental strain CP50 through electroporation. *C. parapsilosis* strain was grown overnight
10 (ON) at 30°C in 5 ml of YPD broth. The following day cells were washed and suspended
11 in 2 ml TE pH 7.5 supplemented with 10 mM Lithium Acetate and 60 µl of DTT 1M. After
12 1h incubation at 30°C with shaking, *Candida* cells were washed twice with ice-cold water
13 and once with sorbitol 1M. The electro-competent pellet was then resuspended in 400 µl of
14 sorbitol 1M and kept on ice. 5 µg of pRibo plasmid and 5 µg of the corresponding RT were
15 mixed with 40 µl of competent *Candida* cells. Electroporation was performed using 0.2 cm
16 cuvettes (Cell Projects Ltd, Harrietsham, United Kingdom) and Bio-Rad Gene Pulser (Bio-
17 Rad, Hercules, USA), set at 1.8 kV, 25 µFD and 200 Ω. Following electroporation, cells
18 were let recover for 3h at 30°C under static condition and then plated onto YPD-Nou agar
19 plates.

20 *CpALS4770* and *CpALS4780* transformed clones were screened by allele-specific PCR
21 using primers 4770_EF/4770mut_R and 4780mut_F/4780R (Supplementary Table 1),
22 respectively, recognizing the edited sequences. Genomic DNA (gDNA) from *C.*
23 *parapsilosis* colonies that resulted positive by colony PCR screening was extracted. Q5
24 High-Fidelity DNA polymerase (New England Biolabs) was used to perform the PCR
25 reaction using primers 4770EF/4770R for *CpALS4770* and 4780EF/4780R for *CpALS4780*
26 (Supplementary Table1). Purified DNA fragments were then digested with KpnI (New
27 England Biolabs) and sequenced (LIGHTRUN, GATC-Biotech, Konstanz, Germany).

28

29 **2.6 Growth ability and pseudohyphal formation**

30 The growth ability of *C. parapsilosis* edited strains was compared to their respective
31 parental wild-type strains in YPD liquid media at 37°C. Briefly, a single colony for each
32 strain was inoculated in 10 ml of YPD broth and incubated ON at 30°C with shaking.
33 Following 18 h incubation, the optical density was measured at 600nm (OD₆₀₀) with a

1 spectrophotometer (Biophotometer, Eppendorf, Hamburg, Germany) and suspensions were
2 diluted in 100 ml YPD in order to reach an OD₆₀₀ of 0.1. *C. parapsilosis* strains were
3 incubated at 37°C with shaking (220 rpm) and optical density was measured each hour in
4 disposable cuvettes (10 mm path length) (Kartell Labware, Noviglio, Italy).
5 The panel of *C. parapsilosis* mutant strains obtained in this study and the wild-type strain
6 was analyzed for their ability to undergo morphogenesis under inducing condition (YPD
7 broth supplemented with 10% FBS) according to a previously standardized protocol
8 (Bertini et al., 2016).

9

10 **2.7 Biofilm formation assay on plastic surfaces**

11 Biofilm formation by *C. parapsilosis* strains was evaluated as previously described
12 (Tavanti et al., 2007). Briefly, strains were grown in SAB broth at 30°C, and the
13 concentration of each suspension, microscopically determined, was adjusted to 1.5×10^7
14 cell/ml. Twenty microliters of yeast suspension were added to 180 µl of SAB broth
15 supplemented with 8% glucose in a 96-well (round bottom) polystyrene microtiter plate
16 (Corning, New York, USA). Following a 24h incubation, biofilm biomass was evaluated
17 by spectrophotometric measurement, determining optical density of both biofilm matrix
18 and sessile cells embedded in the matrix. To this end, 100 µl PBS were added to each well
19 and optical density at 405 nm (OD₄₀₅) was measured using an automated plate reader
20 (Microplate Reader 550, Bio-Rad). Mean background values (negative control wells) were
21 subtracted from the mean value obtained for biofilm formed by each strain. Biofilm
22 biomass was expressed as biofilm biomass index (ratio between the OD₄₀₅ detected for the
23 edited strain and the OD₄₀₅ detected for CP50).

24 The cellular metabolic activity was evaluated by the XTT/menadione assay (Ramage et al.,
25 2001). Briefly, a 0.5 g/l XTT (Sigma-Aldrich) solution in PBS was mixed with a 1 µM
26 menadione (Sigma-Aldrich) solution in acetone. An aliquot of 100 µl of XTT/menadione
27 solution was added to each well and incubated in the dark at 37°C. Following a 2 h
28 incubation, 80 µl of the supernatant were then transferred into a new 96-well plate to
29 measure colorimetric development at 490 nm (OD₄₉₀). Background optical density of
30 negative control wells was subtracted from the mean value obtained from each strain and
31 metabolic activity was expressed as biofilm metabolic index (ratio between the OD₄₉₀
32 detected for the edited strain and the OD₄₉₀ detected for CP50).

33

1 **2.8 Biofilm formation on glass beads and scanning electron microscopy (SEM)**
2 **imaging**

3 For biofilm formation on glass beads, overnight yeast suspension was diluted in SAB broth
4 supplemented with 8% glucose (final concentration $10^5 \times \text{CFU/ml}$) and incubated in the
5 presence of porous sintered glass beads (ROBU®, Germany) at 37°C for 24 h. The ratio
6 between beads and diluted yeast suspension was 1 bead:1 mL. The presence of attached
7 cells to the glass beads was evaluated by CFUs counting after the sonication of the beads.
8 First, each bead was washed three times with 1ml sterile sodium-phosphate buffer (PBS) to
9 remove unbound yeasts and placed in a 2ml-eppendorf tube containing 1ml of fresh PBS.
10 Then, samples were vortexed for 30 seconds and sonicated in a BactoSonic ultrasound bath
11 (BANDELIN electronic GmbH & Co. KG, Germany) for 1 minute, followed by an
12 additional 30 seconds vortexing. Ten-fold serial dilutions of the sonication fluid were
13 plated onto Sabouraud agar plates and the plates were incubated for 24 h at 30 °C for
14 colony counting. For SEM imaging, yeast biofilms were grown on porous glass beads as
15 described above. Afterwards, all beads were washed in ddH₂O to remove unbound fungal
16 cells and fixed for 24h at 4°C (4% paraformaldehyde, 2.5 % glutaraldehyde in 0.05 M
17 HEPES). Subsequently, the samples were dehydrated in 30, 50, 70, 90, 95, 100% ethanol,
18 critical point dried, mounted on aluminium stubs, sputter coated with a 20 nm layer of gold
19 palladium and examined in the SEM (ZEISS 1530 Gemini, Carl Zeiss Microscopy GbmH,
20 Germany) operating using the in-lens electron detector. For picture processing images have
21 been cropped, adjusted for optimal brightness and contrast (applied to the whole image)
22 using Photoshop Lightroom (Adobe Systems, San Jose, Ca, USA).

23

24 **2.9 Adhesion to human buccal epithelial cells (HBECs)**

25 Adhesive properties of the mutant and wild-type strains were evaluated according to
26 previously standardize method (Bertini et al., 2013; Bertini et al., 2016; Zoppo et al.,
27 2018). Yeast cells were grown in YPD medium ON at 30°C, collected by centrifugation,
28 washed and resuspended in PBS (pH 7.4) at a density of 1×10^8 cells/ml. Similarly,
29 HBECs were washed in PBS (pH 7.4) then adjusted to a density of 1.0×10^5 cells/ml.
30 HBECs and yeast cells were co-incubated at a ratio of 1:1000 for 45 min at 37°C with
31 gentle shaking. Buccal cells were then collected by filtration through polycarbonate filters
32 (pore diameter of 12 µm, Millipore), gram stained and examined by light microscopy at
33 1000× magnification. The number of yeast adherent to 100 HBECs was counted. At least
34 three independent experiments were performed; in each experiment, co-incubation of yeast

1 cells and HBECs was performed in triplicate The donor of exfoliated buccal cells signed
2 an informed consent in accordance with the Declaration of Helsinki. Local ethical
3 Committee (Committee on Bioethics of the University of Pisa) approval was received for
4 this set of experiments (Ref. no. 6/2019, Prot. No. 0012910/2019).

5

6 **2.10 Gene expression analysis by real-time RT-PCR**

7 Transcriptional levels of *C. parapsilosis* *ALS* genes were evaluated by real-time reverse
8 transcription PCR (RT-PCR) from total RNA. Each strain was inoculated in 10 ml of YPD
9 at 30°C ON and 500 µl of this suspension were inoculated in 20 ml of YPD for 24 h at
10 30°C. Cells were recovered by centrifugation at 4500 rpm for 5 min and washed twice with
11 10 ml of PBS and total RNA was extracted from 5×10^7 cells using Nucleospin RNA
12 (Machery Nagel, Düren, Germany), according to manufacturer's instructions.
13 Spectrophotometric analysis, using UVette® (10 mm path length, Eppendorf, Milan, Italy),
14 was used to determine the quantity of extracted RNA and to check for the presence of
15 protein contamination. cDNA was synthesized, with random primers, using 0,7-1 µg of
16 total RNA as template, through the Reverse Transcription System kit (Promega, Madison,
17 USA), following manufacturer's instructions. Gene expression levels were analyzed by
18 real-time PCR, using primers CPAG_05054NF/CPAG_05054NR for *CpALS4790*,
19 CPAG_05056F/CPAG_05056R for *CpALS4800*, CPAG_05314F/CPAG_05314R for
20 *CpALS660*, CPAG_00368F/CPAG_00368R for *CpALS4770*, CPAG_00369F
21 /CPAG_00369R for *CpALS4780* and lastly ACT1_RT/ACT2_RT for actin, used as
22 reference housekeeping gene (Table 2.2). SsoAdvanced™ universal SYBR Green
23 supermix (Bio- Rad, Hercules, USA) was used to perform the Real-time PCR in 96 well
24 plates on CFX96 Touch Real-Time PCR Detection System (Bio-Rad, Hercules, USA),
25 following manufacturer's instruction. Each primer pair produced a single amplicon with a
26 uniform melting curve. The transcription level of detected genes was calculated using the
27 formula of $2^{-\Delta\Delta Ct}$ (Bertini et al., 2016; Zoppo et al., 2018; Lombardi et al., 2019b).

28

29 **2.11 Murine model of vaginal candidiasis**

30 The pathogenicity of *C. parapsilosis* parental and edited strains was tested in a murine
31 model of vaginal candidiasis. *In vivo* experiments were conducted following the ethical
32 protocol approved by the committees on the Ethics of Animal Experiments of the "Istituto
33 Superiore di Sanità", Rome, Italy (Permit number: DM 227/2016-B dated 22/12/2016).

1 Briefly, groups of 5 BALB/c mice were intravaginally inoculated with a 1×10^6 yeast/20
2 μ l. Fungal vaginal burden was monitored over an infection period of 3 weeks. 100 μ l of
3 undiluted and serially diluted vaginal fluids, taken at designated times (0, 1, 2, 5, 7, 14 and
4 21 days), were seeded, in triplicate, onto chloramphenicol (50 mg/L) supplemented
5 Sabouraud dextrose agar plates. Cultures were incubated at 30°C for 48-72 h.

6

7 **2.12 Statistical analysis**

8 Statistical analysis of mean adhesion was performed using GraphPad Prism software
9 (version 6.05 for Windows, La Jolla, CA USA). One-way ANOVA followed by
10 Bonferroni's post-hoc test was used to evaluate the differences in biofilm formation,
11 adhesion ability, gene expression levels and CFU values obtained in murine infection
12 experiments. A P value <0.05 was considered statistically significant.

13

1 **3. RESULTS**

2

3 **3.1 Screening and identification of *C. parapsilosis* *CpALS4770* and *CpALS4780* edited**
4 **clones**

5 An episomal CRISPR/Cas9 strategy was used in order to inactivate *CpALS4770* and
6 *CpALS4780* genes using the *C. parapsilosis* highly adhesive clinical isolate CP50 as
7 parental strain. Screening was performed by allele specific PCR using primers
8 4780mut_F/4770R recognizing the correct editing of the *CpALS4780* gRNA according to
9 the repair template used yielding a PCR product of 428 bp (Supplementary Fig. 1A).

10 The genotype of *C. parapsilosis* clones that resulted positive by colony PCR screening was
11 confirmed by restriction analysis. As shown in Fig. 1A, the PCR product obtained with
12 primers 4780EF/4780R (1400 bp) was digested with KpnI generating two fragments of
13 993 bp and 407 bp. This result confirms the correct editing of the *CpALS4780* gene,
14 attesting the presence of a KpnI site and therefore, the use of the repair template RT-4780
15 for the repair of the DBS induced by Cas9 (Fig. 1A). Among all the clones resulted
16 positive to the restriction analysis one clone was selected for sequencing of the gRNA
17 region. Sequencing results obtained with primers 4780EF/4780R confirmed the expected
18 genotype, with the insertion of two stop codons and a KpnI restriction site in the coding
19 sequence of *CpALS4780* mutant strain (Fig. 1B). The edited strain was named CP50-
20 ed4780.

21 CP50 and the single edited strain CP50-ed4780, were used as parental strains for the
22 creation of *CpALS4770* single and double edited strains, respectively. Edited clones were
23 screened by allele specific PCR using primers 4770_EF/4770mut_R. A DNA band of the
24 expected molecular weight (372 bp) was obtained for all genomic backgrounds used
25 (Supplementary Fig. 1B). Amplification with primers 404770_EF/404770R and
26 subsequent digestion of the PCR product (914 bp) with KpnI generated DNA bands with
27 the expected molecular weight (363 bp and 551 bp) (Fig. 1C). These results attest the
28 correct integration of the repair template RT-4770 in *CpALS4770*. Sequencing of the
29 gRNA region obtained with primers 4770EFF/4770R (Fig. 1D) confirmed the expected
30 genotype. As a result, the edited strains obtain from CP50 and CP50-ed4770 parental
31 strains were named CP50-ed4770 and CP50-ed4770/4780, respectively.

32

33 **3.2 Effect of *CpALS4770* and *CpALS4780* gene inactivation on growth ability and *in***
34 ***vitro* morphological properties of *C. parapsilosis***

1 The impact of the inactivation of genes encoding for cell wall anchored proteins on *C.*
2 *parapsilosis* growth ability was evaluated in YPD medium at 37°C for 24 hours. The graph
3 shown in Fig. 2A shows the results obtained for parental strain CP50, CP50-ed4770,
4 CP50-ed4780, CP50-ed4770/4780. Growth curves obtained from the individual strains
5 indicate no difference between the wild-type and edited strains of *C. parapsilosis*.

6 Fungal cell morphology of CP50 strain and related mutant strains (CP50-ed4770, CP50-
7 ed4780, CP50-ed4770/4780) grown in SAB or YPD media at 37°C was observed with
8 bright field light microscopy. As shown in Fig. 2B, which reproduces representative
9 micrographs of each strain grown in SAB, CP50 and CP50-ed4780 presented a typical *C.*
10 *parapsilosis* round morphology. Interestingly, CP50-ed4770/4780 and, to a lesser extent
11 CP50-ed4770, produced elongated cells which tended to form cellular aggregates that were
12 particularly evident in the case of the double mutant strain. When grown in YPD medium,
13 only CP50-ed4770/4780, but not CP50-ed4770, showed slightly elongated cells and a mild
14 tendency to form cellular aggregates (Figure 2C).

15 Unlike *C. albicans*, *C. parapsilosis* is unable to form true hyphae, but under inducing
16 conditions, such as incubation at 37°C and the presence of serum, cells produce elongated
17 forms with constrictions at the cell-cell junctions, also known as pseudohyphae. As
18 illustrated in Fig. 2C, after 24h at 37°C in YPD broth supplemented with 10% FBS, all the
19 edited *C. parapsilosis* strains were equally able to form pseudohyphae, demonstrating that
20 inactivation of *CpALS4770* and *CpALS4780* or both genes contextually did not affect
21 morphogenesis. **When grown in YPD medium, the double CP50-ed4770/4780 mutant**
22 **strain, and to a lesser extent Cp50-ed4770, produced elongated cells, which tended to form**
23 **cellular aggregates, even in the absence of FBS (Fig. 2C).**

24

25 **3.3 Impact of *CpALS4770* and *CpALS4780* editing on *C. parapsilosis* ability to form** 26 **biofilm on abiotic surfaces.**

27 Biofilm formation assays were set up to evaluate the ability of all the edited strains
28 obtained in this study to produce biofilm on abiotic surfaces, such as plastic surfaces and
29 glass beads. Biofilm production on plastic surfaces was performed in 96-well microtiter
30 plates in the presence of SAB supplemented with 8% glucose. Following 24h incubation at
31 37°C, biofilm formation was evaluated assessing both biofilm cellular density and cellular
32 metabolic activity. As illustrated in Fig. 3A, while CP50-ed4780 produced the same extent
33 of biofilm as the parental strain, CP50-ed4770 showed a marked reduction in its ability to
34 form biofilm as compared to its parental strain. Surprisingly, the double edited strain

1 CP50-ed4770/4780 displayed a higher capacity to produce biofilm as compared to the
2 wild-type strain. Metabolic activity results (Fig. 3B) confirmed the trend observed for
3 biomass data.

4 Biofilm production by the panel of parental and mutant strains was also evaluated on glass
5 beads. *C. parapsilosis* wild type and edited strains were grown in SAB broth supplemented
6 with 8% glucose and incubated at 37°C for 24 h in the presence of glass beads. Fig. 4
7 shows the biofilm produced by *C. parapsilosis* parental and edited strains on glass beads
8 using SEM microscopy. As shown in Figure 4, *C. parapsilosis* single mutant strains,
9 CP50-ed4770 (Fig.4C-D) and CP50-ed4780 (Fig.4E-F), and double mutant strain CP50-
10 ed4770/4780 (Fig.4G-H), adhered and produced biofilm on glass beads to the same extent
11 as the wild-type strain (A-B). No significant differences were observed in CFU number of
12 wild type and mutant strains dislodged from biofilm under these experimental conditions
13 (data not shown).

14

15 **3.5 Inactivation of *CpALS4770* and *CpALS4780* differently affects the adhesion** 16 **properties of *C. parapsilosis* on human buccal epithelial cells (HEBCs)**

17 An *in vitro* adhesion assay to HBECs was used to evaluate the adhesive properties of the
18 mutant and parental strains, in order to better understand the role played by *CpALS4770*
19 and *CpALS4780* in *C. parapsilosis* adhesion to host surfaces.

20 As illustrated in Fig. 5, *CpALS4770* gene editing caused a reduced ability of *C.*
21 *parapsilosis* mutant strain to adhere to HBECs cells as compared to the parental strains
22 (3,9-fold reduction). Conversely, *CpALS4780* gene editing did not affect the adhesion of *C.*
23 *parapsilosis* to HBEC. Interestingly, the simultaneous inactivation of *CpALS4770* and
24 *CpALS4780* resulted in an enhanced ability of *C. parapsilosis* to adhere on HBECs. As
25 shown in Fig. 5, the double mutant strain CP50-ed4770/4780 showed a hyper-adhesive
26 phenotype, with a 2,6-fold increase in the adhesion index as compared to the
27 corresponding parental strain ($P < 0.0001$, one-way ANOVA followed by Bonferroni's *post-*
28 *hoc* test). Such a hyper-adhesive phenotype observed for the mutant strains also correlated
29 with a marked tendency to form cellular aggregates, as also visible from the micrographs
30 shown in Fig. 5, below the histograms.

31

32 **3.6 *ALS* gene expression profiles in *CpALS4770* and *CpALS4780* gene edited strains**

33 To evaluate how the lack of functional *CpAls4770p* and *CpAls4780p* impacts on the
34 expression profile of *CpALS* genes, quantitative gene expression analysis was performed

1 on *C. parapsilosis* wild type and mutant strains. *C. parapsilosis* strains were grown in YPD
2 medium and in the same *in vitro* conditions used for preparation of fungal suspensions in
3 HBEC adhesion assays. As shown in Fig. 6, in the experimental conditions tested, reduced
4 levels of *CpALS4780* and *CpALS4800* mRNA were observed in CP50-ed4770. In contrast,
5 CP50-ed4780 mutant strain did not show differences in the expression level of any *CpALS*
6 gene. Notably, an overexpression of *CpALS4780* was detected in the CP50 double mutant
7 strain. Even with marked trends detected, the results obtained did not reach the level of
8 statistical significance, due to the high experimental variability observed.

9

10 **3.11 *In-vivo* model of vaginal infection**

11 The pathogenic potential of the *C. parapsilosis* parental and edited strains was assessed in
12 an *in-vivo* model of murine vaginal candidiasis. Following vaginal challenge, BALB/c
13 mice were monitored for fungal vaginal burden over an infection period of 3 weeks. As
14 shown in Fig. 7, the number of CFUs recovered from mice infected with CP50-ed4770,
15 CP50-ed4780 and CP50-ed4770/4780 was significantly lower with respect to those
16 recovered from wild type (CP50). Differently from CP50-ed4780 and CP50- ed4770/4780
17 where this trend was maintained throughout the entire course of the vaginal monitoring,
18 reduction of CP50-ed4770 recovered from infected mice was statistically significant only
19 in the early stages of the infection, while significance was lost at late time-points. These
20 findings suggest that the lack of CpAls4770p or CpAls4780p or their simultaneous
21 inactivation results in a significant reduced ability to colonize and persist on the vaginal
22 mucosa.

23

24 **4. DISCUSSION**

25

26 In this study we described the inactivation of two functionally uncharacterized *ALS* genes
27 of *C. parapsilosis*, *CpALS4770* and *CpALS4780*. The episomal CRISPR/Cas9 system
28 (Lombardi et al., 2017) and a repair template carrying two stop codons were used for the
29 successful creation of single edited strains (CP50-ed4770, CP50-ed4780) in *C.*
30 *parapsilosis* CP50 strain, a clinical isolate previously characterized as highly adhesive to
31 HBECs (Bertini et al., 2013) and a double edited strain (CP50-ed4770/4780) generated in
32 CP50-ed4780 genetic background.

33 Microscopical analysis of edited and parental strains indicated a tendency for CP50-
34 ed4770 and CP50- ed4770/4780 strains to form elongated cells and to produce cellular

1 aggregates when grown in Sabouraud broth. This phenotype was conserved in YPD
2 medium for CP50-ed4770/4780, but not for CP50-ed4770. This cellular behaviour, which
3 was more pronounced in the double mutant strain, was also observed by Zhao and
4 colleagues in *C. albicans* *ALS5*, *ALS6* or *ALS7* knock-out strains (Zhao et al., 2007). A
5 possible explanation could reside in the structural rearrangements of the fungal cell-wall
6 proteins that occur in response to the lack of functional CpAls4770 and CpAls4780
7 proteins resulting in the exposure of other adhesive moieties on the *C. parapsilosis*
8 surfaces.

9 Phenotypic analysis of wild type and edited strains confirmed that the deletion of
10 *CpALS4770* and *CpALS4780* did not affect the growth rate of the yeast in YPD medium.
11 Since in *C. albicans* *ALS* genes are associated with hyphal formation (Hoyer et al., 1998;
12 Argimón et al., 2007), a morphogenesis assay was used to evaluate the effect of the
13 inactivation of *CpALS4770*, *CpALS4780* or both in the ability of *C. parapsilosis* strains to
14 produce pseudohyphae. All mutant strains were able to undergo morphogenesis under
15 inducing conditions, indicating that neither *CpALS4770* nor *CpALS4780* play a major role
16 in this process. This finding is in agreement with results previously observed for *C.*
17 *parapsilosis* deletion of *CpALS4800* and for *C. orthopsilosis* *CoALS4210* inactivation
18 (Zoppo et al., 2018). A biofilm formation assay (Ramage et al., 2001; Tavanti et al., 2007)
19 was used to investigate a possible role for *CpALS4770* and *CpALS4780* in *C. parapsilosis*
20 biofilm formation process, as previously reported for *ALS3* in *C. albicans* (Nobile et al.,
21 2006). Both CP50 and CP50-ed4780 strains were able to produce biofilm with the same
22 extent while CP50-ed4770 had a statistically significant reduction in both biofilm biomass
23 and metabolic activity. Notably, the double *CpALS4770/CpALS4780* mutant displayed a
24 marked increase in biofilm production as compared to wild type strain. These results
25 indicate that, while *CpALS4770* seems to be important in biofilm formation, *CpALS4780*
26 does not appear to be directly implicated in this process. The peculiar phenotype of CP50-
27 ed4770/4780 could be explained by the up-regulation of other members of the *ALS* gene
28 family resulting in a more adherent strain. Alternatively, the lack of CpAls4770p and
29 CpAls4780p may also have caused an alteration of the cell-wall structure organization that
30 exposes other adhesive moieties of the *C. parapsilosis* surfaces, resulting in an increased
31 aggregative phenotype. As supported by SEM analysis, a minimum extent of biofilm
32 formation could be detected on glass beads for all *C. parapsilosis* parental and edited
33 strains; however, no difference was observed between the wild type and edited strains
34 biofilm production. The involvement of *C. albicans* Als proteins on the adhesion to glass

1 surfaces has been already described by Aoki and colleagues (Aoki et al., 2012) through
2 heterologous expression experiments performed in *Saccharomyces cerevisiae*. In this
3 study, each *ALS* gene was found to contribute to the adhesion on glass surfaces. Therefore,
4 the effect of the inactivation of *CpALS4770* and *CpALS4780* on glass beads biofilm could
5 have been masked by the adhesion ability of the remaining *ALS* genes of *C. parapsilosis*.
6 The role of *CpALS4770* and *CpALS4780* in the adhesion of *C. parapsilosis* to biotic
7 surfaces was assessed in an *in vitro* model, of co-incubation of yeast cells in the presence
8 of human buccal epithelial cells (HBECs) (Bertini et al., 2013; Bertini et al., 2016; Zoppo
9 et al., 2018). While *CpALS4770* seemed not to be involved in the adhesion of *C.*
10 *parapsilosis* to epithelial human surfaces, a reduction in the adhesion ability of CP50-
11 ed4770 mutant strains if compared with their relative parental strain was observed.
12 Similarly to what observed in biofilm production assays, the contextual inactivation of
13 *CpALS4770* and *CpALS4780* resulted in significantly increased adhesion to HBECs. Such
14 peculiar phenotype was already described by Zhao and co-workers (Zhao et al., 2007)
15 when adhesion of *C. albicans* mutant strains of *ALS5*, *ALS6* or *ALS7* was tested on human
16 vascular endothelial cell monolayers and buccal epithelial cells. As previously mentioned
17 for biofilm formation, this finding could be linked to a re-organization of the cell-wall
18 structure or to an up-regulation of other *ALS* genes in the double mutant.
19 To verify the last hypothesis, the transcription levels of *C. parapsilosis ALS* genes were
20 evaluated through real-time RT-PCR in wild type and mutant strains. Even though the
21 alterations in expression levels were conserved in all three independent experiments, no
22 difference reached statistical significance, due to experimental variability. However, CP50-
23 ed4770 showed a reduction in *CpALS4790* and *CpALS4800* mRNA levels, which could at
24 least partially explain the reduced adhesion ability observed with the HBECs assay. Both
25 *CpALS4800* (Bertini et al., 2016) and *CpALS4790* (unpublished results) are in fact required
26 for the adhesion of *C. parapsilosis* to buccal epithelium. Moreover, the double mutant
27 strain, CP50-ed4770/4780, displayed a 27-fold overexpression of *CpALS4780*, suggesting
28 an attempt of *C. parapsilosis* to overcome the presence of truncated CpAls4780 protein. In
29 *C. albicans* it has been shown that *ALS1* overexpression leads to extensive flocculation and
30 an aggregative phenotype (Huang, 2012). In this case, the only overexpressed gene in the
31 double mutant strain is the edited *CpALS4780*, which produces a non-functional adhesin.
32 Since this truncated protein encompasses only the first 185 amino acids, we can exclude
33 the possibility that the amyloid-forming region (AFR) is responsible for the aggregative
34 phenotype observed in the double mutant strain (Garcia et al., 2011; Oh et al., 2019). A

1 proteomic analysis of the cell wall structure of single and double edited strains coupled
2 with a measurement of hydrophobic forces involved in cell adhesion by atomic force
3 microscopy (AFM) may help to elucidate the observed phenotype (El-Kirat-Chatel et al.,
4 2015).

5 Finally, data obtained from the murine model of vaginal candidiasis clearly indicated that
6 the single or contextual deletion of these genes causes a significant reduction in the ability
7 of *C. parapsilosis* to persist in the vaginal mucosa, compared with the wild type strain. To
8 conclude, these findings confirm that both *CpALS4770* and *CpALS4780* contribute to the
9 pathogenesis of murine vaginal candidiasis.

10

11 **Acknowledgments**

12 We are thankful to Geraldine Butler for providing plasmids pUC57_HH_HDV_sgADE2b
13 and pSAT1. We are grateful to Dr. Colin G. Egan (CE Medical Writing, Pisa, Italy) for
14 revising the manuscript for English language.

15

16 **Funding**

17 This work was supported by the University of Pisa (grant no. PRA_2017_18 n°18). The
18 authors declare no conflict of interest.

19

20

REFERENCES

- Aoki W, Kitahara N, Miura N, Morisaka H, Kuroda K, Ueda M. 2012. Profiling of adhesive properties of the agglutinin-like sequence (ALS) protein family, a virulent attribute of *Candida albicans*. *FEMS Immunol Med Microbiol*;65(1):121-4.
- Argimón S, Wishart JA, Leng R, Macaskill S, Mavor A, Alexandris T, Nicholls S, Knight AW, Enjalbert B, Walmsley R, Odds FC, Gow NAR, Brown AJP. 2007. Developmental Regulation of an Adhesin Gene during Cellular Morphogenesis in the Fungal Pathogen *Candida albicans*. *Eukaryotic Cell*;6(4):682-692.
- Bertini A, De Bernardis F, Hensgens LA, Sandini S, Senesi S, Tavanti A. 2013. Comparison of *Candida parapsilosis*, *Candida orthopsilosis*, and *Candida metapsilosis* adhesive properties and pathogenicity. *Int J Med Microbiol*;303(2):98-103.
- Bertini A, Zoppo M, Lombardi L, Rizzato C, De Carolis E, Vella A, Torelli R, Sanguinetti M, Tavanti A. 2016. Targeted gene disruption in *Candida parapsilosis* demonstrates a role for CPAR2_404800 in adhesion to a biotic surface and in a murine model of ascending urinary tract infection. *Virulence*;7(2):85-97.
- Butler G, Rasmussen MD, Lin MF, Santos MA, Sakthikumar S, Munro CA, Rheinbay E, Grabherr M, Forche A, Reedy JL, Agrafioti I, Arnaud MB, Bates S, Brown AJ, Brunke S, Costanzo MC, Fitzpatrick DA, de Groot PW, Harris D, Hoyer LL, Hube B, Klis FM, Kodira C, Lennard N, Logue ME, Martin R, Neiman AM, Nikolaou E, Quail MA, Quinn J, Santos MC, Schmitzberger FF, Sherlock G, Shah P, Silverstein KA, Skrzypek MS, Soll D, Staggs R, Stansfield I, Stumpf MP, Sudbery PE, Srikantha T, Zeng Q, Berman J, Berriman M, Heitman J, Gow NA, Lorenz MC, Birren BW, Kellis M, Cuomo CA. 2009. Evolution of pathogenicity and sexual reproduction in eight *Candida* genomes. *Nature*;459(7247):657-62.
- Cota EHoyer LL. 2015. The *Candida albicans* agglutinin-like sequence family of adhesins: functional insights gained from structural analysis. *Future Microbiol*;10(10):1635-548.
- Doench JG, Fusi N, Sullender M, Hegde M, Vaimberg EW, Donovan KF, Smith I, Tothova Z, Wilen C, Orchard R, Virgin HW, Listgarten J, Root DE. 2016. Optimized sgRNA design to maximize activity and minimize off-target effects of CRISPR-Cas9. *Nat Biotechnol*;34(2):184-191.
- El-Kirat-Chatel S, Beaussart A, Derclaye S, Alsteens D, Kucharikova S, Van Dijck P, Dufrene YF. 2015. Force nanoscopy of hydrophobic interactions in the fungal pathogen *Candida glabrata*. *ACS nano*;9(2):1648-55.

- Enkler L, Richer D, Marchand AL, Ferrandon D, Jossinet F. 2016. Genome engineering in the yeast pathogen *Candida glabrata* using the CRISPR-Cas9 system. *Sci Rep*;6:35766.
- Gao Y, Zhao Y. 2014. Self-processing of ribozyme-flanked RNAs into guide RNAs in vitro and in vivo for CRISPR-mediated genome editing. *J Integr Plant Biol*;56(4):343-9.
- Garcia MC, Lee JT, Ramsook CB, Alsteens D, Dufrêne YF, Lipke PN. 2011. A role for amyloid in cell aggregation and biofilm formation. *PLoS One*;6(3):e17632-e17632.
- Grahl N, Demers EG, Crocker AW, Hogan DA. 2017. Use of RNA-Protein Complexes for Genome Editing in Non-albicans *Candida* Species. *mSphere*;2(3).
- Hoyer LL, Fundyga R, Hecht JE, Kapteyn JC, Klis FM, Arnold J. 2001. Characterization of agglutinin-like sequence genes from non-albicans *Candida* and phylogenetic analysis of the ALS family. *Genetics*;157(4):1555-67.
- Hoyer LL, Payne TL, Bell M, Myers AM, Scherer S. 1998. *Candida albicans* ALS3 and insights into the nature of the ALS gene family. *Curr Genet*;33(6):451-9.
- Huang G. 2012. Regulation of phenotypic transitions in the fungal pathogen *Candida albicans*. *Virulence*;3(3):251-61.
- Lombardi L, Oliveira-Pacheco J, Butler G. 2019a. Plasmid-Based CRISPR-Cas9 Gene Editing in Multiple *Candida* Species. *mSphere*;4(2).
- Lombardi L, Turner SA, Zhao F, Butler G. 2017. Gene editing in clinical isolates of *Candida parapsilosis* using CRISPR/Cas9. *Sci Rep*;7(1):8051.
- Lombardi L, Zoppo M, Rizzato C, Bottai D, Hernandez AG, Hoyer LL, Tavanti A. 2019b. Characterization of the *Candida orthopsilosis* agglutinin-like sequence (ALS) genes. *PLoS One*;14(4):e0215912.
- Morio F, Lombardi L, Binder U, Loge C, Robert E, Graessle D, Bodin M, Lass-Flörl C, Butler G, Le Pape P. 2019. Precise genome editing using a CRISPR-Cas9 method highlights the role of CoERG11 amino acid substitutions in azole resistance in *Candida orthopsilosis*. *J Antimicrob Chemother*;74(8):2230-2238.
- Neale MN, Glass KA, Longley SJ, Kim DJ, Laforce-Nesbitt SS, Wortzel JD, Shaw SK, Bliss JM. 2018. Role of the Inducible Adhesin CpAls7 in Binding of *Candida parapsilosis* to the Extracellular Matrix under Fluid Shear. *Infect Immun*;86(4):e00892-17.

- Nobile CJ, Andes DR, Nett JE, Smith FJ, Yue F, Phan QT, Edwards JE, Filler SG, Mitchell AP. 2006. Critical role of Bcr1-dependent adhesins in *C. albicans* biofilm formation in vitro and in vivo. *PLoS Pathog*;2(7):e63.
- Norton EL, Sherwood RK, Bennett RJ. 2017. Development of a CRISPR-Cas9 System for Efficient Genome Editing of *Candida lusitanae*. *mSphere*;2(3).
- Oh S-H, Smith B, Miller AN, Staker B, Fields C, Hernandez A, Hoyer LL. 2019. Agglutinin-Like Sequence (ALS) Genes in the *Candida parapsilosis* Species Complex: Blurring the Boundaries Between Gene Families That Encode Cell-Wall Proteins. *Frontiers in microbiology*;10(781).
- Ramage G, Vande Walle K, Wickes BL, Lopez-Ribot JL. 2001. Standardized method for in vitro antifungal susceptibility testing of *Candida albicans* biofilms. *Antimicrob Agents Chemother*;45(9):2475-9.
- Tavanti A, Hensgens LA, Ghelardi E, Campa M, Senesi S. 2007. Genotyping of *Candida orthopsilosis* clinical isolates by amplification fragment length polymorphism reveals genetic diversity among independent isolates and strain maintenance within patients. *J Clin Microbiol*;45(5):1455-62.
- Vyas VK, Barrasa MI, Fink GR. 2015. A *Candida albicans* CRISPR system permits genetic engineering of essential genes and gene families. *Sci Adv*;1(3):e1500248.
- Zhao X, Oh SH, Hoyer LL. 2007. Deletion of ALS5, ALS6 or ALS7 increases adhesion of *Candida albicans* to human vascular endothelial and buccal epithelial cells. *Med Mycol*;45(5):429-34.
- Zhu M, Sun L, Lu X, Zong H, Zhuge B. 2019. Establishment of a transient CRISPR-Cas9 genome editing system in *Candida glycerinogenes* for co-production of ethanol and xylonic acid. *J Biosci Bioeng*;128(3):283-289.
- Zoppo M, Lombardi L, Rizzato C, Lupetti A, Bottai D, Papp C, Gacser A, Tavanti A. 2018. CORT0C04210 is required for *Candida orthopsilosis* adhesion to human buccal cells. *Fungal Genet Biol*;120:19-29.

Supplementary Table 1: Primer sequences used in this study.

Primer	Sequence 5' →3'	Usage
Generation of pRIBO-sgCpALS4770 and pRIBO-sgCpALS4780		
GA7_pUC57F (Lombardi et al., 2017)	TTTAGAGCTAGAAATAGCAAGTTAA AATAAGGCTA GTCC	Linearization of pUC57_HH_HDV_sgA DE2B
GA7_pUC57R (Lombardi et al., 2017)	GAATTTGGAAAAGAAAGAAAGAAA GAAGGAAGG AAGG	Linearization of pUC57_HH_HDV_sgA DE2B
TOP sgRNA Cp4770	TTCTTTCTTTTCCAAATTCAGTGCTT CTGATGAGTCCGTGAGGACGAAAC GAGTAAGCTCGTC	Generation of the <i>CpALS4770</i> sgRNA
BOTTOM sgRNA Cp4770	GCTATTTCTAGCTCTAAAACCGTTT ATTGCCTTTGTGCTTGACGAGCTTA CTCGTTTCGT	Generation of the <i>CpALS4770</i> sgRNA
TOP sgRNA CPAR2_4780	TTCTTTCTTTTCCAAATTCAGCCTCC CTGATGAGTCCGTGAGGACGAAAC GAGTAAGCTCGTC	Generation of the <i>CpALS4780</i> sgRNA
BOTTOM sgRNA CPAR2_4780	GCTATTTCTAGCTCTAAAACGGGTT GGTATTGGAGCCTCCGACGAGCTTA CTCGTTTCGT	Generation of the <i>CpALS4780</i> sgRNA
GA_pSAT1_F (Lombardi et al., 2017)	CAGTGAATTGGAGATCGGTACTTCG GTACTTTGGTGTA ACTGG	Amplification of the ribozyme cassette
GA_pSAT1_R (Lombardi et al., 2017)	GTGTACCGGTATCTCGACGCATTCG CTTTATTTATAAACTCATATACGAA AAATATATAAAAC	Amplification of the ribozyme cassette
Repair template synthesis		
RT_2xSTOP_CPAR2_4 770 F *	CCACAAATCCAATGATTAAACAATT ATCATTGCC TAATAGGGTACC TT	<i>CpALS4770</i> repair template synthesis
RT_2xSTOP_CPAR2_4 770 R *	TGCTTGAACGAAGGTTGTAAGCACA AAGGCAATAAA GGTACCCTATTA	<i>CpALS4770</i> repair template synthesis
RT_2xSTOP_CPAR2_4 780 F *	ACCACTGCAAACCTCCAAGGAGGCT CCAATACCAAC TAATAGGGTACC	<i>CpALS4780</i> repair template synthesis
RT_2xSTOP_CPAR2_4 780 R *	ACACGATTGTTGAAGACAATGTTAT TAGTTGATGTG GTACCCTATTAGT	<i>CpALS4780</i> repair template synthesis
Screening and sequencing of edited clones		
4770_EF	CACCTCCTTTACGGCATTGT	<i>CpALS4770</i> sequencing
4770R	TGCTGTATACGATATCTTCG	<i>CpALS4771</i> sequencing

4770mut_R	ACAAAGGCGGTACCTTACTA	<i>CpALS4770</i> allele specific PCR
4780mut_F	CAATACCAACTAATAGGGTACC	<i>CpALS4780</i> allele specific PCR
4780R	CTCCCCATTTTATTGATTGTGAG	<i>CpALS4780</i> sequencing
4780EF	CCAACCTCGTGGATTGCTTCT	<i>CpALS4780</i> sequencing
Real-time PCR		
CPAG_00368F	TGTCCTCGACAACCTCCAGCTT	<i>CpALS4770</i> real-time amplification
CPAG_00368R	GGTTCTAAAATGGGTGGAATGG	<i>CpALS4770</i> real-time amplification
CPAG_00369F	AACGTCCAACAGGTCAAGTG	<i>CpALS4780</i> real-time amplification
CPAG_00369R	CTCCCCATTTTATTGATTGTGAG	<i>CpALS4780</i> real-time amplification
CPAG_05054NF	TCGAGTTCCTAATGGTGCAG	<i>CpALS4790</i> real-time amplification
CPAG_05054NR	CCTTCTTCACCCCAGTTTTG	<i>CpALS4790</i> real-time amplification
CPAG_05314F	GGGATCAGCAAATTCTGTCGA	<i>CpALS660</i> real-time amplification
CPAG_05314R	CCAGCGGTAAAACATTGGGA	<i>CpALS660</i> real-time amplification
CPAG_05056F	AAAGTCACCACCACCGAGGTT	<i>CpALS4800</i> real-time amplification
CPAG_05056R	CGGCGCAGATGTGCTAATG	<i>CpALS4800</i> real-time amplification
ACT1_RT	AGTGTGACTTGGATGTCAGAAAGG AATTGT	Actin real-time amplification
ACT2_RT	ACAGAGTATTTTCTTTCTGGTGGAG CA	Actin real-time amplification

*: Stop codons are in red and bold; KpnI restriction site is highlighted in yellow.

FIGURE LEGENDS

Supplementary Fig. 1: Screening of *CpALS4770* and *CpALS4780* edited clones. **A)** Screening of *C. parapsilosis CpALS4780* recombinant clones obtained using CP50 as parental strain. Correct editing of the *CpALS4780* was evaluated by allele specific PCR using primers 4780mut_F/4780R. The upper panel shows a schematic representation of wild type and edited *CpALS4780* gene, primer position and expected molecular weight (428 bp) of the PCR product. The lower panel shows the PCR result. 1-14: recombinant clones; 15: CP50 gDNA; NC: negative control (no gDNA); M: 1Kb Gene Ruler 1kb DNA ladder (Thermo Scientific). **B)** Screening of *C. parapsilosis CpALS4770* recombinant clones obtained using CP50 and CP50-ed4780 as parental strains. Correct editing of the *CpALS4770* was evaluated by allele specific PCR using primers 4770_EF/4770mut_R. The upper panel shows a schematic representation of wild type and edited *CpALS4770* gene, primer position and expected molecular weight (372 bp). The lower panel shows the PCR result. 1-5: recombinant clones obtained using CP50 as parental strain; 6-10: recombinant clones obtained using CP50-ed4780 as parental strain ; 11: CP50 gDNA; NC: negative control (no gDNA); M: 1Kb Gene Ruler™ 1kb DNA ladder (Thermo Scientific).

Fig. 1: KpnI restriction analysis and sequencing of *CpALS4780* and *CpALS4770* transformant clones. **A)** *CpALS4780* gRNA region was amplified in the parental strain (CP50) and transformant clones with primers 4780EF/4780R yielding a PCR product of 1400 bp. As shown in the electrophoresis gel, digestion with KpnI generates two fragments of 993 bp and 407 bp, respectively, only if the DSB caused by Cas9 is repaired using RT-4780. M: 1Kb Gene Ruler 1kb DNA ladder (Thermo Scientific); 1: KpnI digestion products of *CpALS4780* gRNA region obtained from putative edited clone; 2: KpnI digestion product of *CpALS4780* gRNA region obtain from CP50 parental strain. **B)** Sequencing results of *CpALS4780* locus confirmed the presence of two stop codons (TAA and TAG) and the KpnI site (GTTACC) allowing the identification of the CP50-ed4780 edited strain. **C)** *CpALS4770* gRNA region was amplified with primers 4770EF/4770R yielding a PCR product of 914 bp. KpnI digestion led to the generation of two fragments of 551 bp and 363 bp only if the DSB caused by Cas9 is repaired using RT-4770. M: 1Kb Gene Ruler 1kb DNA ladder (Thermo Scientific); 1: KpnI digestion product of *CpALS4770* gRNA region obtained from ATCC 22019; 2, 3, 4: KpnI digestion products of *CpALS4780* gRNA region obtained from putative edited *CpALS4770* and *CpALS4770/ CpALS4780* clones, respectively. **D)** Sequencing

results of *CpALS4770 locus* confirmed the presence of two stop codons (TAA and TAG) and the KpnI site (GTTACC) allowing the identification of CP50-ed4770 and CP50ed4770/4780 strains.

Fig. 2: Growth abilities and morphogenesis. **A)** Growth ability of parental and edited strain. Growth curves of CP50, CP50-ed4770, CP50-ed4780, CP50-ed4770/4780 strains in YPD medium at 37°C. **B)** Optical microscopy imaging of CP50 and edited strains. Pictures were taken *from C. parapsilosis* wild type and edited clones grown for 24 h in Sabouraud broth at 37°C. Scale bars denote 10 µm. **C)** Production of pseudohyphae by the panel of edited strains. *C. albicans* SC5314 was included as positive control for filamentation (true hyphae). Morphogenesis was induced in YPD broth in presence of 10% FBS. Following 24 h of incubation at 37°C, 10 µl of each culture was directly observed with an optical microscope at 400 × magnification. Scale bars denote 10 µm.

Figure 3: Evaluation of biofilm formation in the panel of reference and edited *C. parapsilosis* strains obtained in his study. **A)** Total biofilm biomass determined by measuring optical density at 405 nm, following an incubation in Sabouraud+8% glucose for 24 h at 37°C; **B)** Cellular metabolic activity was measured with the XTT/menadione assay, with colorimetric development measured at 490 nm on biofilm formed as described for biomass evaluation. Error bars represent standard error of means of 2 independent experiments, each performed in at least eight replicates. One-way ANOVA followed by Bonferroni's post-hoc test was used to evaluate differences biofilm formation (***: P<0.001; **: P<0.01).

Fig. 4: SEM microscopy performed on biofilm produced on glass beads.

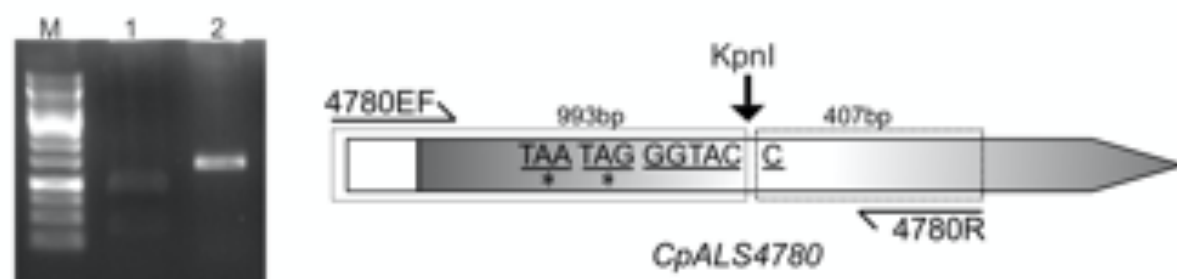
Each panel shows *C. parapsilosis* parental and edited strains adherent to glass beads surfaces. Left column: (overview images) biofilm grown between sintered glass particles of the glass bead. Scale bars denote 20 µm. Right column: (close-up images) *C. parapsilosis* cells with varying amounts of network-like extracellular matrix. Scale bars denotes 2 µm. CP50 (A, B); CP50-ed4770 (B, C); CP50-ed4780 (E, F); EP50-4770/4780 (G, H).

Fig. 5: Evaluation of the adhesive properties of reference and edited *C. parapsilosis* strains to HBECs. Adhesive properties of the *C. parapsilosis* edited strains obtained in this study are compared to their corresponding parental strain. Bars represent adhesion index mean ± standard error of mean. At least three biological replicates were used; ***: P<0.001; **: P<0.01. Micrographs below bars show representative Gram-stained *C. parapsilosis* yeast cells from each strain adhered to a buccal cell observed at a magnification of 1000 ×. Scale bars denote 10 µm.

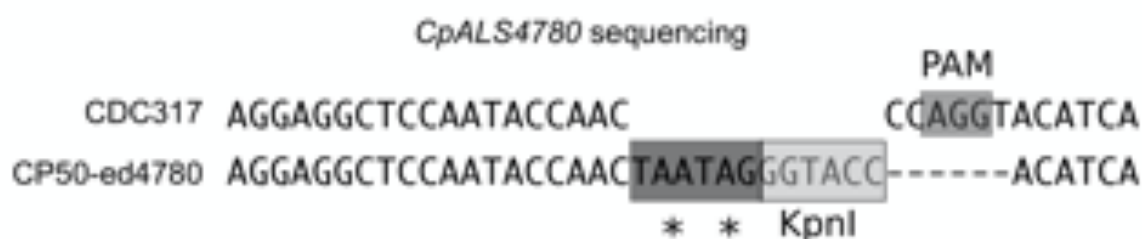
Fig. 6: Transcriptional levels of *CpALS* genes in *C. parapsilosis* CP50, CP50-ed4770, CP50-ed4780 and CP50-ed4770/4780 strains (A-E). Relative expression of each gene in edited strains is normalized on actin and expressed as relative to wild-type values. Error bars represent standard error of three independent experiments, each performed in triplicate. *: P<0.05

Fig.7: Time course of murine vaginal candidiasis. Five BALB/c mice for each strain (CP50, CP50-ed4770, CP50-ed4780, CP50-ed4770/4780) were intra-vaginally infected with 10⁶×cells/20 µl. Bars represent mean values ± standard error of the mean of *C. parapsilosis* CFUs recovered from vaginal fluids at different time points. *P<0.05; **P< 0.01, ***P< 0.001.

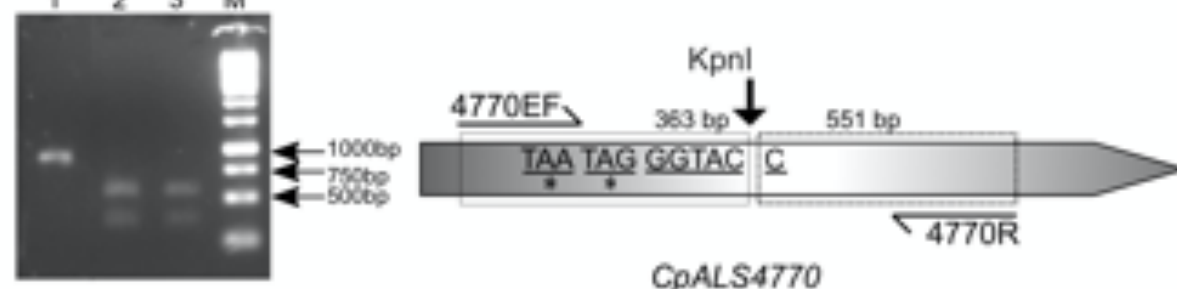
A)



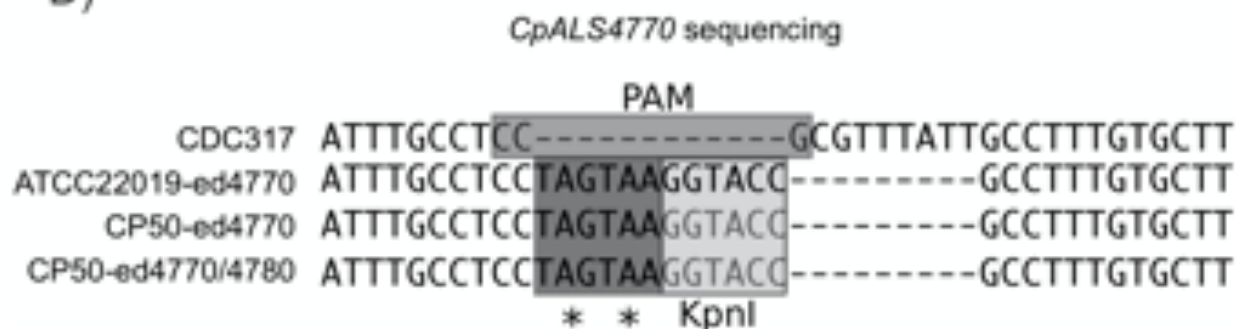
B)

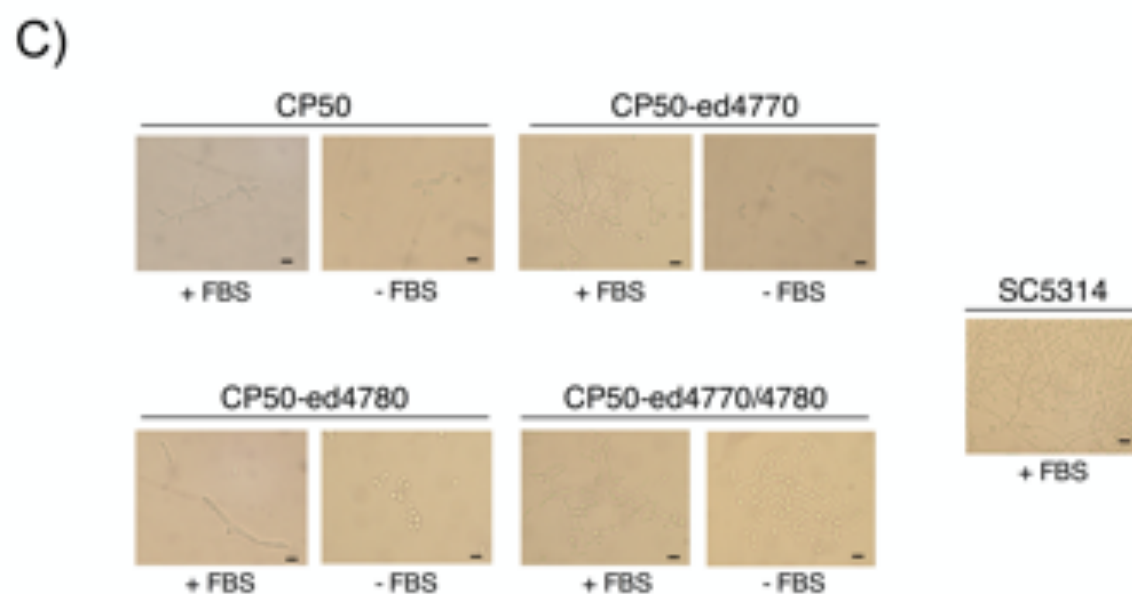
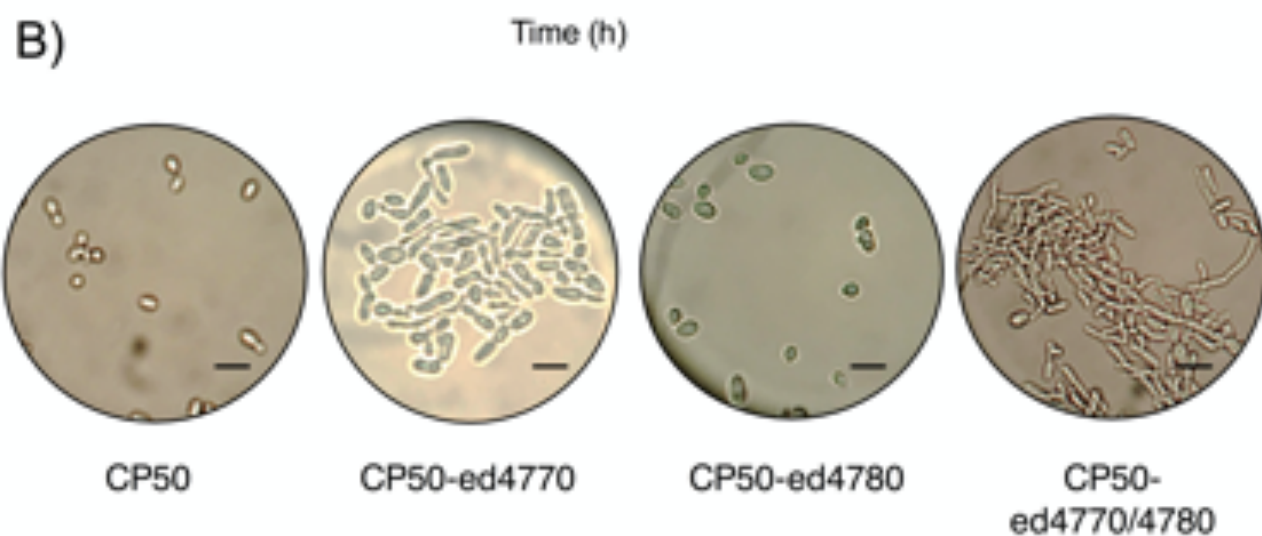
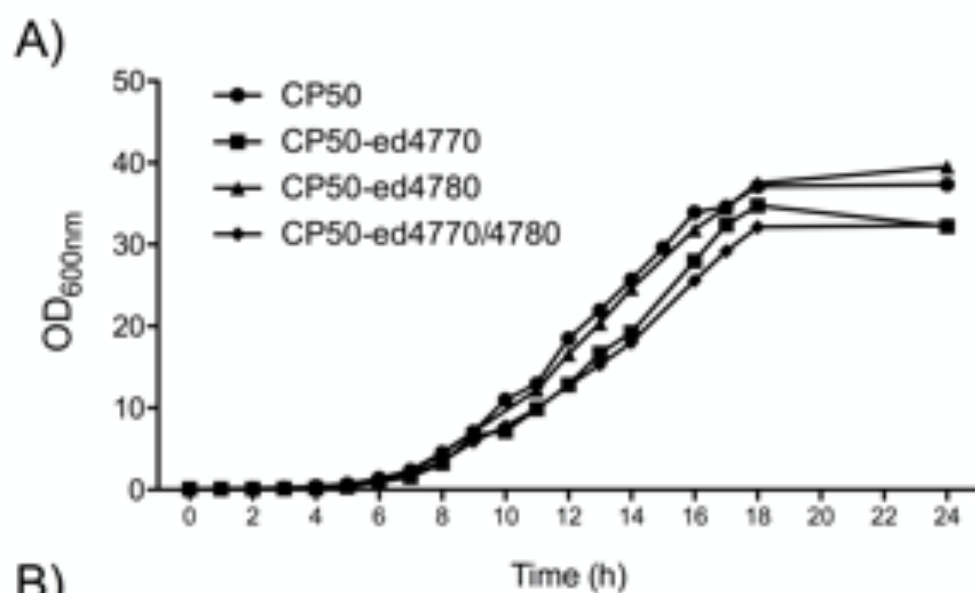


C)

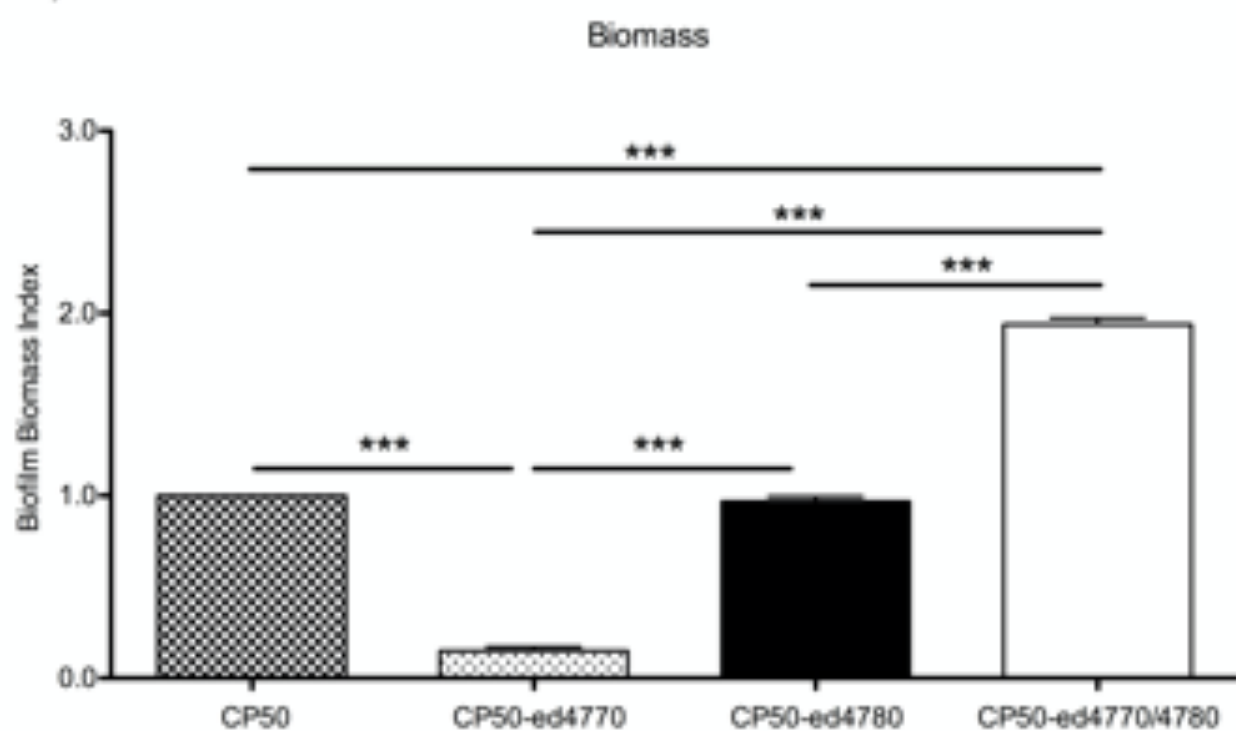


D)

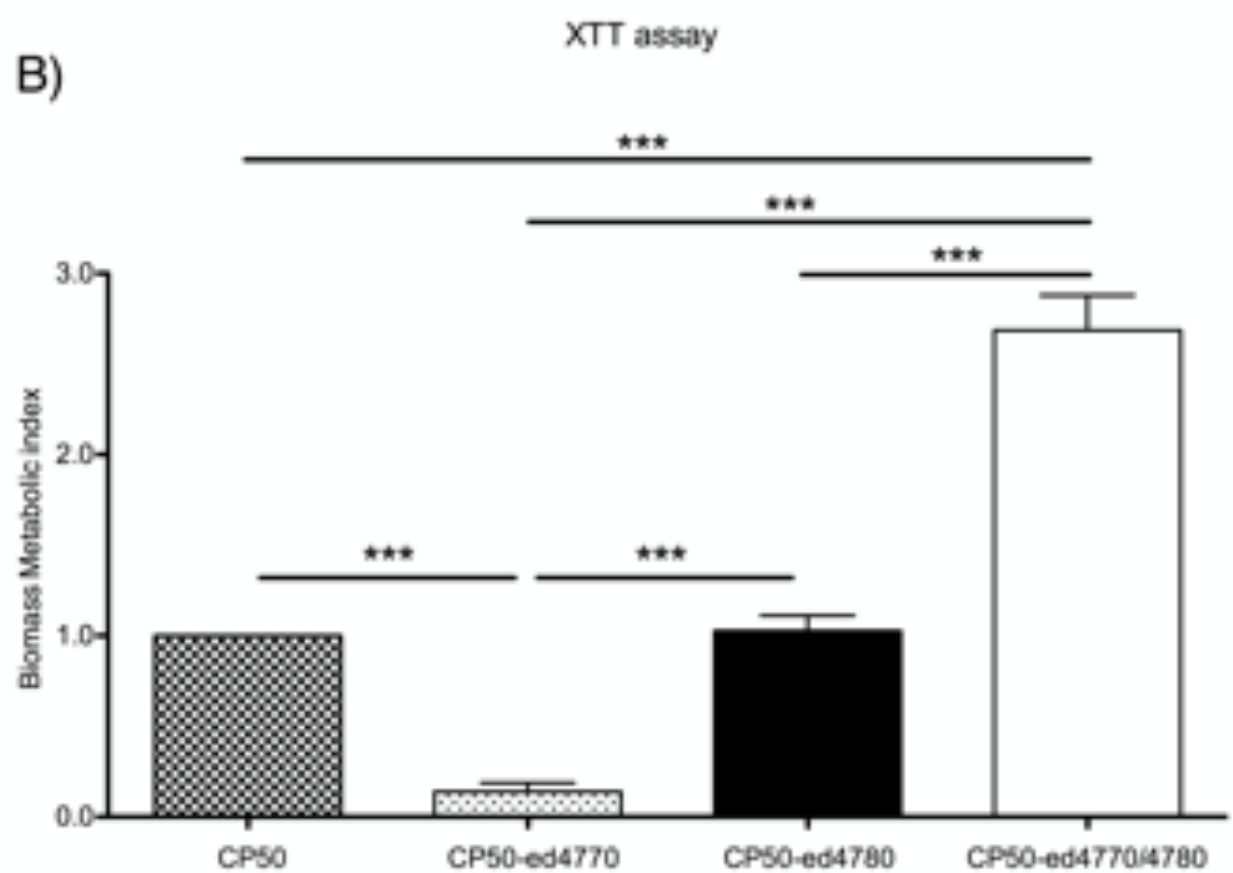


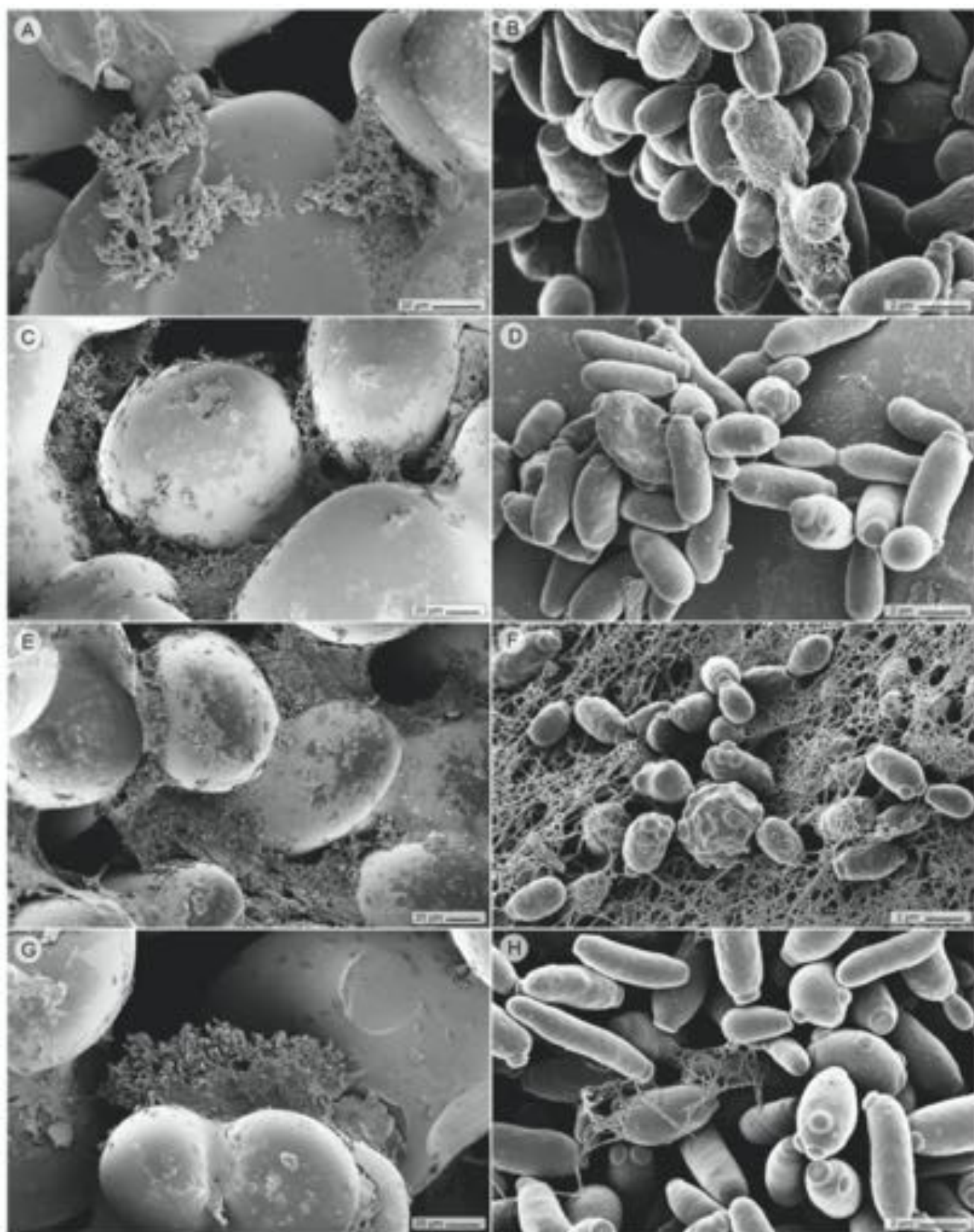


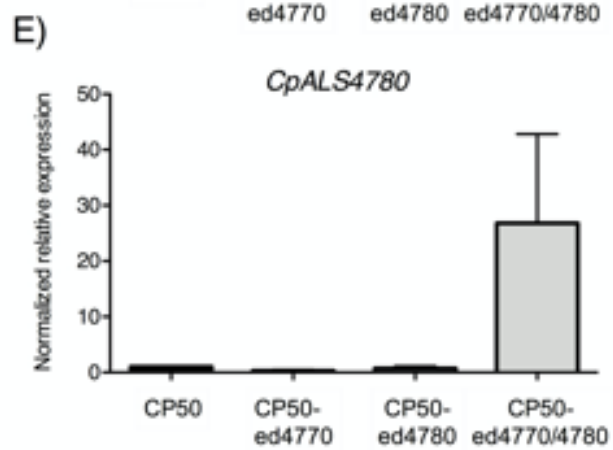
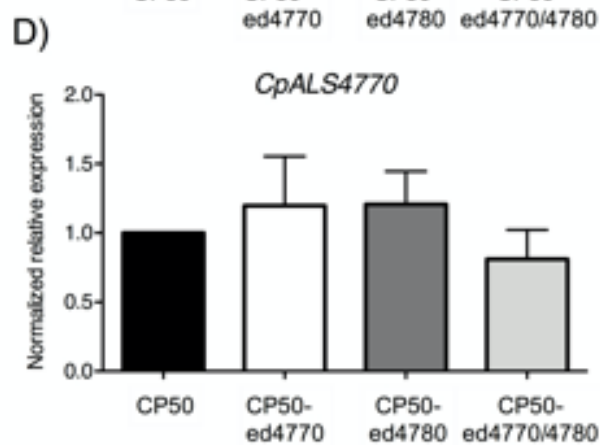
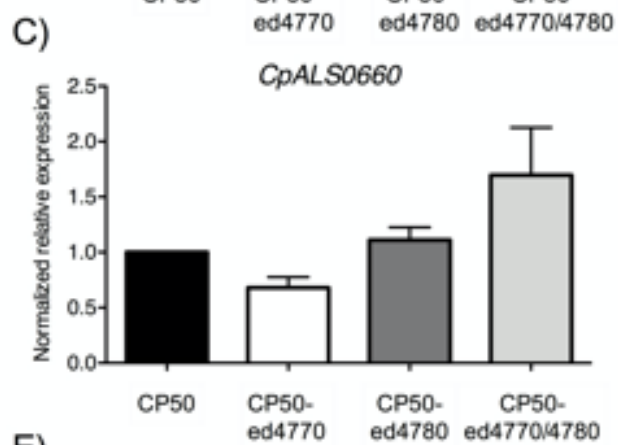
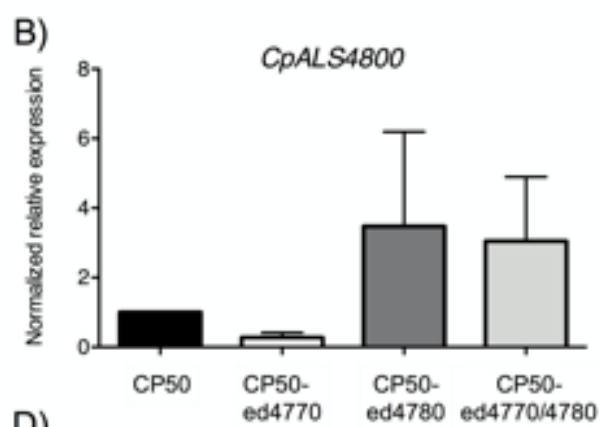
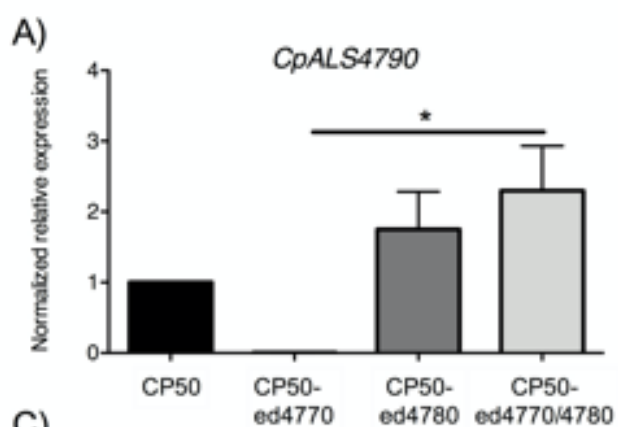
A)

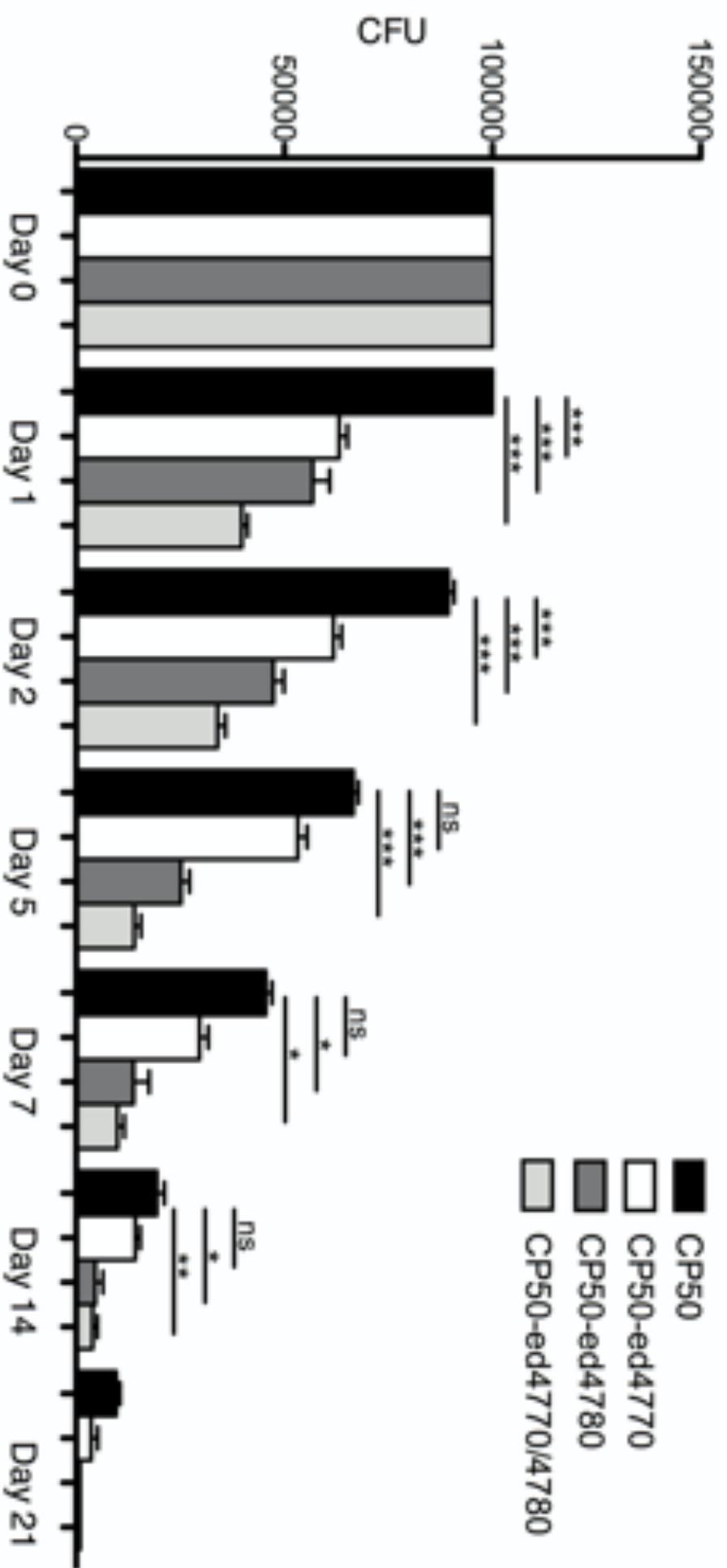


B)

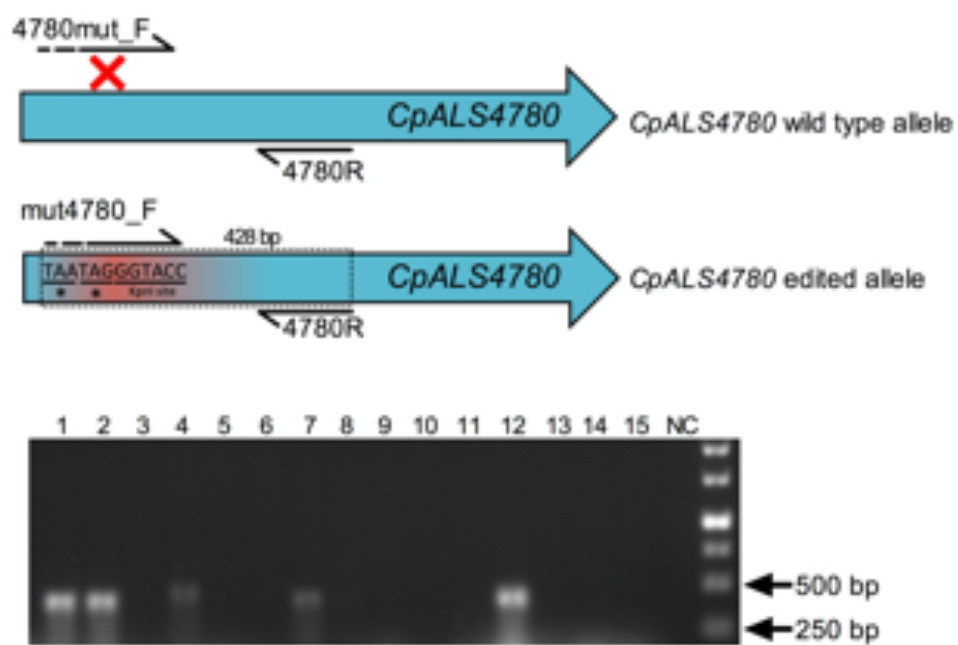








A)



B)

